Progress In Electromagnetics Research B, Vol. 46, 59–78, 2013

MUTUAL COUPLING IN LONGITUDINAL ARRAYS OF COMPOUND SLOTS

Ignacio Montesinos-Ortego[1, *], Manuel Sierra-Pérez[1], Miao Zhang[2], Jiro Hirokawa[2], and Makoto Ando[2]

[1]Grupo de Radiación, ETSI Telecomunicación, Univesidad Politécnica de Madrid, 30 Complutense Ave., Madrid 28040, Spain

[2]Ando and Hirokawa Laboratory, Tokyo Institute of Technology, 2-12-1-S3-19, O-okayama, Meguro-ku, Tokyo 152-8552, Japan

Abstract—The arrays of compound-slots (inclined and displaced from waveguide centre) are not so common in the literature and the existing systematic method of design does not take into account the presence of surrounding elements. For this kind of slots, the reasons why the Elliott's procedure cannot be applied are physically explained. A new method based on circuit theory and scattering matrices connection to include the effects of the external mutual coupling in compound slots arrays is presented in this paper. To certify the validity of the complete technique, the performance of various designed arrays are compared to the results given by full-wave commercial solvers.

1. INTRODUCTION

Electromagnetic coupling between antennas within an array constitutes one of the more concerned problems for the antenna engineer. It causes the antenna to be untuned from the desired design frequency and an alteration of the radiation pattern. Mutual coupling characterization and effects depend on the structure of the antenna and working frequency, so that ad-hoc solutions optimized by iterative processes are normally required.

Focusing on slot array antennas, Elliott in [1, 2] accounts for the external mutual coupling between rectangular waveguide-fed longitudinal slots employing and equivalent array of loaded dipoles, which is particularly useful in the design of small arrays where the mutual coupling is radically different for peripheral and central slots.

Received 8 October 2012, Accepted 15 November 2012, Scheduled 24 November 2012

* Corresponding author: Ignacio Montesinos-Ortego (nacho@gr.ssr.upm.es).

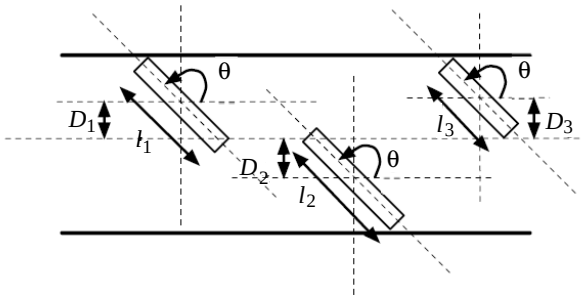

Figure 1. Linear array of parallel compound slots.

To study the behavior of the array inside the guide, Elliott takes advantage of the symmetry of the longitudinal slot and the properties of the electric field at the slot plane to substitute the slots by equivalent shunt elements placed $0.5\lambda_g$ away to each other. Gülick and Elliott demonstrated that this technique is limited, claiming that circuit models based on a single shunt or series element are only valid for standard-height waveguide and/or small offsets [3].

It is Gulick et al. in [4] the first to claim that the idea of a design procedure based on equivalent circuit model must be abandoned since the inclusion of the mutual coupling effect is complex. Instead of using equivalent circuit, Gülick and Elliott proposed integral-equation general technique or the scattering wave study.

Although the first systematic design procedure for linear arrays of parallel compound slots (Fig. 1) was recently proposed by Montesinos et al. in [5, 6], it did not include the effect of surrounding elements. The slots are designed in order to accomplish radiation and impedance requirements, so that they can be different in length and offset (separation from waveguide centre). Rengarajan studied the coupling effect applying the Lorentz Reciprocity Theorem and the Scattering Waves Theory [7]. In this paper, the required procedure to account for the mutual coupling in rectangular-waveguide fed linear array of compound slots is proposed. It constitutes the next stage of the procedure explained in [5, 6] and represents the first attempt of circuit-based mutual coupling characterization employed for compound slot array design.

The main purpose of this kind of array is to be part of two-dimensional waveguide array with linear polarization. By means of radiating compound slots with a common tilting angle, it is possible to polarize the field in the plane where the side-lobe level is the lowest. If the two-dimensional array is squared, a linearly polarized field on

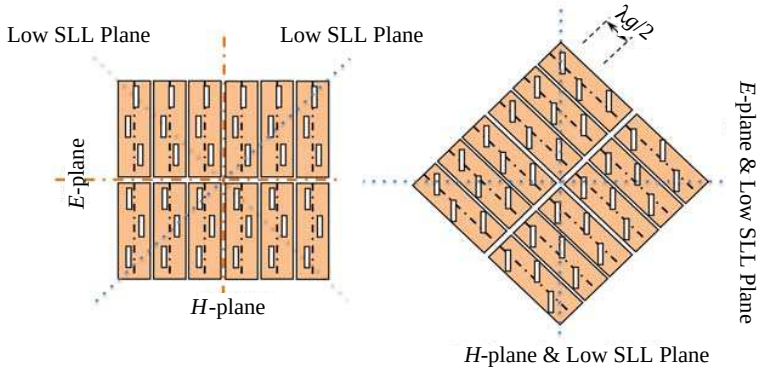

Figure 2. 2D array of parallel longitudinal and parallel compound slots.

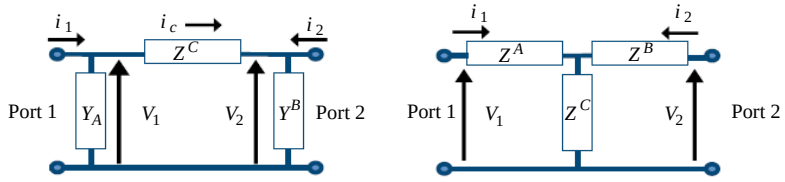

Figure 3. Π and T networks.

the low side-lobe-level planes ($\phi = 45°$ and $\phi = 135°$) will be obtained selecting the tilting angle as $\theta = 45°$, Fig. 2.

This paper is organized as follows: first, the physical explanation of why the Elliot's procedure cannot be applied to the compound slot case is addressed. Secondly, the main effects of the external mutual coupling on the compound slots arrays are presented. After this, the inclusion of the mutual coupling effects into the methodology shown in [5] is explained in detail. Last section compares results with equivalent CST simulations, confirming the validity of the method.

2. SCATTERED WAVES AND EQUIVALENT CIRCUITS FOR COMPOUND SLOTS

The well-known method of slot-array design developed by Elliott is based in two main equations: the first one obtained from the study of the scattering of the feeding waves inside the guide, similar to that of a single shunt admittance. The second one comes from the radiation characteristics of two equivalent and complementary arrays of wired-

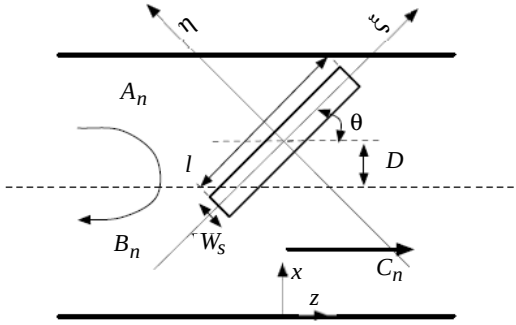

Figure 4. Local coordinate axes.

fed slots and slim dipoles. The connection between both equations is done by equaling the radiated power of the equivalent arrays with the dissipated power by the equivalent shunt element. In this section, the scattered waves inside the waveguide generated when the feeding mode faces a compound slot are analyzed. From this study, the impossibility of modeling the compound slot as a single shunt or series element is stressed out, making the Elliott's procedure not applicable.

First, to physically understand the relation between the voltage in slot terminals and scattered power within the waveguide as a function of the tilting angle θ, the Reciprocity Theorem is applied to the compound slot case. It represents an extension of the analysis performed by Silver and Elliott for longitudinal slot [8, 1]. For the sake of the orientation and size independence, it is convenient to use a locally-defined coordinate system which axis (ξ, η) are placed along the length and width of the slot, Fig. 4.

The term A_n represents the amplitude of the feeding wave. The amplitude of the scattered reflected and transmitted waves, B_n and C_n respectively, were defined by Elliott as:

$$B_n = \frac{\int_{slot} \left(\vec{E}_{slot} \times \vec{H}_{slot}\right) \cdot d\vec{S}}{2 \int_{s_1} \left(\vec{E}_{scat} \times \vec{H}_{scat}\right) \cdot d\vec{S}} \tag{1}$$

$$C_n = \frac{\int_{slot} \left(\vec{E}_{slot} \times \vec{H}_{slot}\right) \cdot d\vec{S}}{2 \int_{s_2} \left(\vec{E}_{scat} \times \vec{H}_{scat}\right) \cdot d\vec{S}} \tag{2}$$

where $\vec{E}_{scat}$ and $\vec{H}_{scat}$ are the scattered fields from the slot and which mathematical expressions can be found in [8, 1].

Considering that all the feeding modes but TE_{10} are under their

cut-off frequency, existing magnetic and electric fields in the slot's aperture are:

$$\vec{H}_{slot} = \vec{\xi}\left(\frac{-j\beta_{10}}{\left(\frac{\pi}{a}\right)}\sin\left(\frac{\pi}{a}x\right)\sin(\theta) + j\cos\left(\frac{\pi}{a}x\right)\cos(\theta)\right)e^{-j\beta_{10}z}$$
$$\vec{E_{slot}} = \frac{V_0}{w}\cos\left(\frac{\pi}{l}\xi\right)\vec{\xi} \tag{3}$$

where β_{10} is the phase constant of the existing mode, a the width of the waveguide, V_0 the voltage at the slot's terminals, and w, l and θ the width, length and inclination angle of the slot.

To obtain the amplitude of backward and forward scattered waves both fields must be described according to the locally defined coordinate system.

$$\begin{aligned}\vec{H}_{slot} =& \vec{\xi}\left(\frac{-j\beta_{10}}{\left(\frac{\pi}{a}\right)}\sin\left(\frac{\pi}{a}\left(D+\frac{a}{2}+\xi\sin(\theta)+\eta\cos(\theta)\right)\right)\sin(\theta)\right.\\ &\left.+ j\cos\left(\frac{\pi}{a}\left(D+\frac{a}{2}+\xi\sin(\theta)+\eta\cos(\theta)\right)\right)\cos(\theta)\right)\\ &e^{-j\beta_{10}(\xi\cdot\cos(\theta)-\eta\cdot\sin(\theta))}\\ \vec{E_{slot}} =& \frac{V_0}{w}\cos\left(\frac{\pi}{l}\xi\right)\vec{\xi}\end{aligned} \tag{4}$$

Substituting (4) into (2), and considering the TE_{10} the single feeding mode $(n = 1, 0)$ one gets

$$\begin{aligned}B_{10} =& \frac{\left(\frac{\pi}{a}\right)^2}{\omega\mu_0\beta_{10}ab}\iint_{slot}\left[\left(\frac{-j\beta_{10}}{\left(\frac{\pi}{a}\right)}\sin\left(\frac{\pi}{a}\left(D+\frac{a}{2}+\xi\sin(\theta)+\eta\cos(\theta)\right)\right)\sin(\theta)\right.\right.\\ &\left.\left.+j\cos\left(\frac{\pi}{a}\left(D+\frac{a}{2}+\xi\sin(\theta)+\eta\cos(\theta)\right)\right)\cos(\theta)\right)\right]\\ &\frac{V_0}{w}\cos\left(\frac{\pi}{l}\xi\right)e^{-j\beta_{10}(\xi\cdot\cos(\theta)-\eta\cdot\sin(\theta))}dS\end{aligned} \tag{5}$$

$$\begin{aligned}C_{10} =& \frac{\left(\frac{\pi}{a}\right)^2}{\omega\mu_0\beta_{10}ab}\iint_{slot}\left[\left(\frac{j\beta_{10}}{\left(\frac{\pi}{a}\right)}\sin\left(\frac{\pi}{a}\left(D+\frac{a}{2}+\xi\sin(\theta)+\eta\cos(\theta)\right)\right)\sin(\theta)\right.\right.\\ &\left.\left.j\cos\left(\frac{\pi}{a}\left(D+\frac{a}{2}+\xi\sin(\theta)+\eta\cos(\theta)\right)\right)\cos(\theta)\right)\right]\\ &\frac{V_0}{w}\cos\left(\frac{\pi}{l}\xi\right)e^{j\beta_{10}(\xi\cdot\cos(\theta)-\eta\cdot\sin(\theta))}dS\end{aligned} \tag{6}$$

Once C_{10} and B_{10} are obtained as a function of the voltage in the slot's aperture, the relation between them will condition the continuity

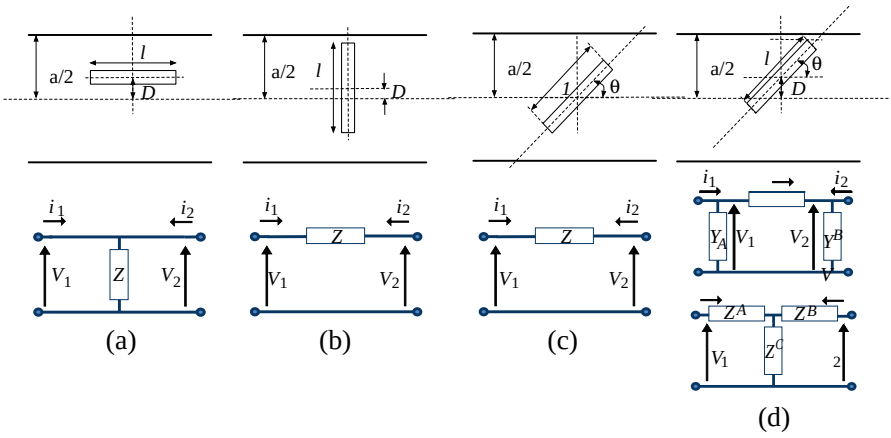

Figure 5. Different slot's configuration and equivalent networks.

of the electric and magnetic field at the plane of its center ($z = 0$). Three cases deserve to be pointed out:

(i) $C_{10} = B_{10}$ the tangential component of the electric field is zero, while the magnetic field in $z = 0^-$ and $z = 0^+$ are in opposite phase. This case squares with an slot parallel to the waveguide axis. With respect to the running mode, the slot behaves like a shunt element in a transmission line, Fig. 5(a).

(ii) $C_{10} = -B_{10}$, forces the tangential component of the electric field to be discontinuous and the magnetic field to show continuity at $z = 0$ plane. In this case, the slot is oriented with its axis perpendicular to the guide axis or it is centered and inclined, and it behaves like a series element in a transmission line, Figs. 5(b) and (c).

(iii) $C_{10} \neq \pm B_{10}$ None of the tangential components of the electric and magnetic fields are continuous nor zero at $z = 0$. This fact causes that the slot cannot be characterized using a single shunt or series element. Since the equivalent currents and voltages are not continuous more complicated schemes are needed, Fig. 5(d).

If a new term $E_{10} = \frac{B_{10}}{C_{10}}$ is defined and its absolute value is plotted for orientations from $\theta = 0°$ to $\theta = 180°$ for five different slot configurations, the three presented cases can be identified in all of the curves, Fig. 6.

Independently of the offset and length values, there are three points where all the graphs converge. For the longitudinal slot ($\theta = 0°$ and $\theta = 180°$) and for the transverse slot ($\theta = 90°$) addressing the first

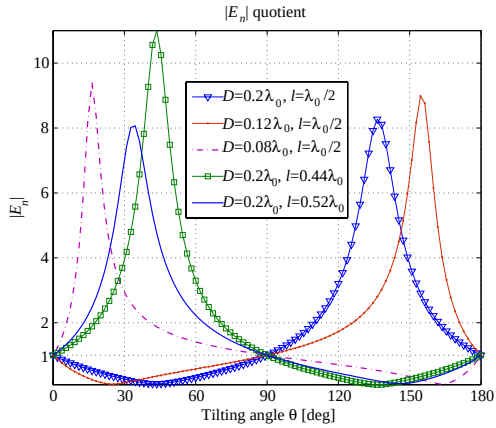

Figure 6. Dependence of E_n with tilting angle.

and the second case, respectively, the absolute value of the ratio E_{10} becomes one. If one goes deeper and the longitudinal or transverse slot is regarded as a two-port device with internal loss (to account for the radiated power), the corresponding impedance matrix can be completely defined with a single complex value.

Away from these specific angles, the ratio between the amplitude of the forward and backward scattered waves depends on the structural parameters like offset and length. Contrary to (i) and (ii), assumptions about the fields in the slot plane can not be done and the corresponding Z matrix is symmetric so it requires three complex values to be univocally defined. This is the case of the compound slot, squaring case (iii).

3. EFFECTS OF THE MUTUAL COUPLING

Some authors of the forties believed that the mutual coupling among longitudinal slots had negligible effects, although Elliott later demonstrated that the presence of the surrounding elements slightly alters the value of the equivalent shunt element. These effects are much more noticeable for the case of compound slots, specially as the tilting angle increases. The main consequences of mutual coupling are degradation of the radiation pattern and a frequency shift in the input matching characteristics. The origin of both is common:

(i) For the first one, due to the existance of surrounding radiators, parasitic electric fields are printed on the aperture of the slots, causing an alteration on the value of the voltage across the

terminals and consequently, the radiated power per each element is different from the ideal case. Normally, this kind of arrays are designed to accomplish an specific symmetric or uniform amplitude tapering. Because of the mutual coupling, the symmetry in feeding is broken so do the side lobes of the radiation pattern. The main lobe direction can be slightly displaced, the side-lobe level increases and the side radiation nulls are filled.

(ii) Since there is a modification on the slot feeding voltage, the magnitude of the scattered fields within the waveguide are thus altered, as it was shown in Eq. (5) and Eq. (6). The amplitude of backward and forward TE_{10} scattered field changes at each slot, generating non-expected forward and backward travelling waves that modify the electric behavior of the global system.

Using the electric circuit theory it is possible to predict these effects on the performance of a given compound slot array. In this paper, the arrays are designed following the procedure described in [5, 6] called *Method of Moments-Forward Matching Procedure* (hereinafter MoM-FMP).

4. COMPLETE DESIGN PROCESS

In [5, 6], the method for serially connecting N compound slots to generate an array did not take into account the influence of the surrounding elements, but an array-equivalent circuit is returned as a preliminary solution. About this array, all the design parameters are known: number of slots, waveguide dimensions and thickness, relative position of radiators, the ideal total radiated power per element and the length of the slots. For the sake of understanding, the different steps to include the effects of mutual coupling in this initial model will be briefly described. Then, along the corresponding subsections the different enumerated points will be explained in detail.

1. The equivalent circuits shown in Fig. 3 allow the exchange of power only inside the waveguide, by means of the feeding mode TE_{10}. The slots' equivalent network and consequently the global array circuit must be modified in such a way it becomes possible to include the effects of the mutual coupling between radiators. At each slot, a new coupling port is defined to account for the externally exchanged power.

2. The physical distribution of the slots and their dimensions are known from the preliminary array, so that an identical array of cable-fed slots embedded in an infinite-large ground plane can be defined. This array is employed to calculate the coupling factor between slots, which is represented as an admittance between every two coupling ports.

3. Inside the array, the coupling factor becomes a N-by-N matrix that relates the generated current at a specific port when there exists a voltage in another terminal. This admittance network is converted into a scattering matrix that represents the coming and going power waves at each coupling port. The new scattering network is connected to the N coupling ports defined in point 1 following the Scattering Network Connection theory [9], which returns the relation between reflected and input power waves at every connection of the circuit. From this, is is easy to calculate the return loss of the whole array and the new radiated power per element once the coupling is included.

4. Knowing this real consumed power per element, the voltage at the slot terminals of the equivalent array and their radiated fields are calculated. The fields are sum in order to obtain the radiation pattern of the array including the mutual coupling between elements.

4.1. New Array Circuit Model

4.1.1. New Slot Model

In [5, 6] networks of two ports and three independent complex elements were used to characterize the behavior of the isolated slot, Fig. 3. A single element was responsible of the radiated power in both T and Π circuits and there was no port included to account for the externally interchanged energy. To achieve this, the general structure of the Π network is kept but a new interface that allows the inclusion of externally coupled power is incorporated, Fig. 7.

The network has changed and its impedance matrix must be accordingly recalculated. Understanding $Z_A = \frac{1}{Y_A}$ and $Z_B = \frac{1}{Y_B}$ one obtains,

$$[Z] = \frac{1}{Z_A + Z_B + Z_C} \begin{bmatrix} Z_A(Z_B + Z_C) & Z_A Z_B & Z_A Z_C \\ Z_A Z_B & Z_B(Z_A + Z_C) & -Z_B Z_C \\ Z_A Z_C & -Z_B Z_C & Z_C(Z_A + Z_B) \end{bmatrix} \quad (7)$$

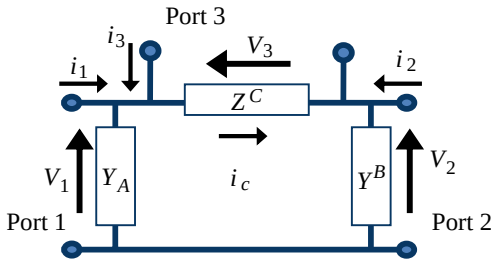

Figure 7. New equivalent network with coupling port.

From the new Z matrix, the S matrix is obtained [10] employing the characteristic impedance of the waveguide as the reference impedance for all the ports. The scattering matrix is vital to the interconnection technique explained in Section 4.2.

4.1.2. Global Circuit and Coupling Model for a N-element Linear Array

The extension of the new model depicted in Fig. 7 to all the elements of the array forces the N-element array to become a circuit of $N+1$ ports (N coupling ports and the original feeding point). Besides the main contribution coming from the feeding wave, the voltage at slot terminals is also dependant of the parasitic field printed on the aperture coming from the radiated fields of the surrounding elements. This contribution directly depends on structural parameters as the relative angle, distance and position between elements as well as the amplitude distribution.

To relate the externally induced current I_i at slot i when the slot j is excited with a voltage V_j, the coupling factor Y_{ij} is defined and mathematically described by the following equation,

$$\begin{bmatrix} I_1 \\ I_2 \\ \vdots \\ I_n \end{bmatrix} = \begin{bmatrix} 0 & Y_{1,2} & \dots & \dots & Y_{1,n} \\ Y_{2,1} & & Y_{2,3} & & \vdots \\ & & \ddots & & \vdots \\ & & & 0 & \\ Y_{n,1} & Y_{n,2} & \dots & Y_{n,n-1} & 0 \end{bmatrix} \begin{bmatrix} V_1 \\ V_2 \\ \vdots \\ V_n \end{bmatrix} \tag{8}$$

The calculus of the coupling factor is performed by means of a complementary array of cable-fed slots which structure and properties are known. The coupling factor is obtained for every pair of apertures as explained in Section 4.1.3, obtaining as a result a N-by-N admittance matrix and its corresponding scattering matrix [10, 11]. The diagonal is completely filled with zeros since these terms represent the self admittance of the slots, already taken into account in the design of the feeding network.

So far, the whole structure can be divided into two main sub-networks, one for modelling the feeding of the slots from the generator and the other to model the coupling through the half-free space region. Both sub-networks are connected as depicted in Fig. 8. According to the method of analysis described in Section 4.2, the return loss at the feeding port (once the mutual coupling effects are included) can be calculated.

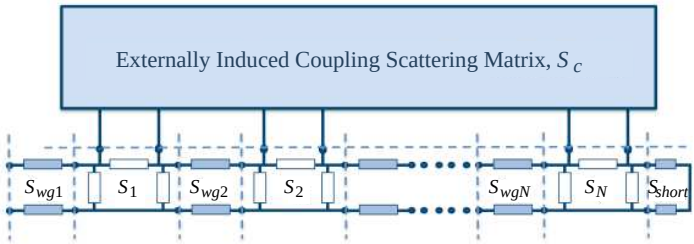

Figure 8. Sub-networks interconnection.

4.1.3. Calculation of the Coupling Factors Y_{ij}

Generally speaking, the mutual coupling between two slots may be strictly calculated performing two double integrals: one to obtain the field radiated by the first slot on the second one, the other to obtain the reaction of the printed field with the current distribution on the aperture of the second aperture. This can be drastically simplified under the condition of narrow slots, since the transverse integrals are replaced by their respective values at the center times the slot width. In [7], a complete study of the accuracy of this approximation is carried out, revealing that error remains insignificant and the coupling expression can be rapidly and accurately evaluated in terms of a numerical single integral.

The initial execution of MoM-FMP returns a waveguide-fed array with a specific distribution of parallel compound slots of different lengths. From this, an identical array of cable-fed slots embedded in an infinite ground plane is generated. Since the ideal radiated power, the physical dimensions and the array distribution are known, the voltage V_j at the terminals of the isolated slots are known and the coupling factor can be mathematically evaluated as explained below.

A generic scenario of coupling between two slots is shown in Fig. 9, which represents a simplification of the model proposed in [7, 12, 13] since the slots are always parallel to each other. The centre of the slot 1 is placed at the origin of the coordinate system zy at $(0, 0, 0)$ and its length is $2l_1$. The second slot is at $(0, y_c, z_c)$ and $2l_2$ long. The width w is the same for both slots and much less than length to keep the condition of narrow slot, $\frac{w}{10} < 2l$.

The formulation presented in [12] is followed to calculate the mutual coupling factor as

$$Y_{21} = -\frac{1}{V_{S_1} V_{S_2}} \iint_{slot2} \left(\vec{H}_{21}^{l} \frac{V_{S_2}}{w} \cos\left(\frac{\pi}{2l_2} z'\right) \hat{y} \right) dz' dy' \qquad (9)$$

where V_{S_1} and V_{S_2} are the voltages at slots terminals specified by

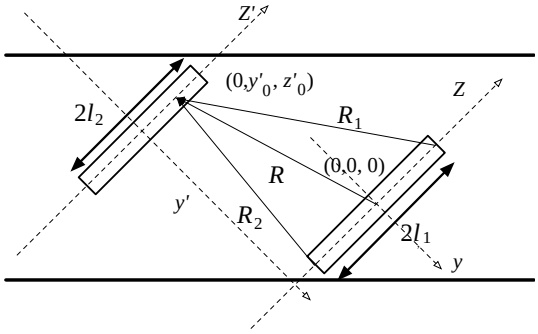

Figure 9. Scheme of the phenomenon.

the desired amplitude tapering; $\vec{H}_{21}^{l}$ is the longitudinal magnetic field generated on the slot 2 by the magnetic current at slot one. To simplify the calculation of $\vec{H}_{21}^{l}$, the distribution of magnetic current in slot one is approximated by a PWS dipole-like distribution, which allows the use of the closed forms developed by Richmond in [14].

$$\vec{H}_{21}^{l} = \frac{1}{j2\pi\eta}\left[\frac{e^{-jkR_1}}{R_1} + \frac{e^{-jkR_2}}{R_2} - 2\cos\left(kl_1\right)\frac{e^{-jkR}}{R}\right]\hat{z}' \qquad (10)$$

$$R = \sqrt{y_c^2 + z_o^2} \quad R_1 = \sqrt{y_c^2 + \left(z_o - l_1\right)^2} \quad R_2 = \sqrt{y_c^2 + \left(z_o + l_1\right)^2}$$

where $k = \frac{2\pi}{\lambda}$, η and λ are the free space impedance and wavelength respectively.

The PWS dipole-like approximation forces the inclusion of a correcting factor for cosinusoidal distribution.

$$\Lambda = \frac{2l1}{\pi}\frac{k}{1 - \cos\left(kl_1\right)} \qquad (11)$$

finally,

$$Y_{21} = -\Lambda \int_{slot2} \vec{H}_{21}^{l} \cos\left(\frac{\pi}{2l_2}z'\right) dz'dy' \qquad (12)$$

A complete discussion of more convenient correction factor is carried out in [12].

The coupling factor Y_{ij} represents the relation between the printed parasitic current in the antenna i due to the presence of a voltage between the terminals of slot j, Fig. 10. Its immediate equivalent circuit model is based on ideal transformers connected to the new coupling ports defined in Subsection 4.1.1. As a result, for an array of N elements a whole N-by-N ports externally induced coupling network is created.

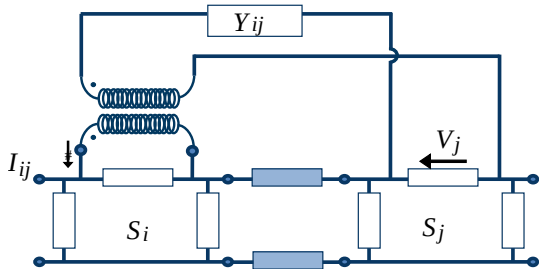

Figure 10. Coupling representation in a 2-element array.

4.2. Feeding and Coupling Matrices Connection

It is now mandatory to analyze the interconnection of the feeding network and the half free space coupling network, independently of the number of elements selected by the designer, the frequency or dimensions of the radiators.

On one hand the distribution, offsets and lengths of the radiators are known from MoM-FMP, as well as the S matrices of every single component of the proposed array: slots, connecting waveguides and short. After the radiating port is included and the S matrix is consequently modified, for an array of N-elements one gets N three-port circuits and N two-port devices relative to the connecting waveguides. The short is regarded as a load, a single-port matrix.

On the other hand, from 4.1.2 the N-by-N scattering matrix of the externally induced coupling equivalent network is calculated. Its ports are connected to the coupling port defined in the feeding network, as it is shown in Fig. 8. Both circuits can be evaluated as a bigger single one, following the Scattering Matrix Connection technique perfectly described in [9].

A N-slot linear array contains a total of $2N+2$ scattering matrices: N for the radiating slots; N for the connecting waveguides; one for the external coupling and one for the short. For the ith component having n_i ports it is possible to define incoming and outgoing wave variables by

$$b_i = S_i a_i \tag{13}$$

valid for all the elements but the independent generator, where an extra component should be included

$$b_g = S_g a_g + c_g \tag{14}$$

where c_g is the wave produced by the generator. If all the equations are written together in a common global system of equation one gets:

$$b = Sa + c \tag{15}$$

where

$$a = \begin{bmatrix} a_1 \\ a_2 \\ \vdots \\ a_m \end{bmatrix}; \quad b = \begin{bmatrix} b_1 \\ b_2 \\ \vdots \\ b_m \end{bmatrix}; \quad c = \begin{bmatrix} c_1 \\ c_2 \\ \vdots \\ c_m \end{bmatrix}; \tag{16}$$

$$S = \begin{bmatrix} S_1 & 0 & \dots & 0 \\ 0 & \ddots & & \\ & & S_i & \vdots \\ & & \ddots & 0 \\ 0 & \dots & 0 & S_m \end{bmatrix} \tag{17}$$

The scattering matrix written in Eq. (17) is a block diagonal matrix whose submatrices are the S matrices of the components of the network in an specific order. Zeros represent null matrices.

Next step consists of the definition of a mathematical expression that specifies how the network is set up. For a pair of connected ports, i and j, it is clear that the incoming wave at port i must equal the outgoing wave at port j, assuming that both are identically normalized. So that, it is possible to define a connection matrix Γ.

$$a_i = b_j \text{ and } a_j = b_i \qquad \begin{bmatrix} b_i \\ b_j \end{bmatrix} = \begin{bmatrix} 0 & 1 \\ 1 & 0 \end{bmatrix} \begin{bmatrix} a_i \\ a_j \end{bmatrix} \tag{18}$$

$$b = \Gamma a \tag{19}$$

Filling up the global S matrix of Eq. (17), and substituting Eq. (19) into Eq. (15), one gets

$$Sa + c = \Gamma a \;\rightarrow c = (\Gamma - S)\, a \tag{20}$$

If the right-hand term is defined as the connection scattering matrix, W, the previous equation can be rewritten as

$$W = \Gamma - S \rightarrow a = W^{-1} c \tag{21}$$

At this point, all the elements of c and W matrices are known, so that the solution of Eq. (21) returns the incoming waves a at all the component ports in the global network. Once a is also known, b is calculated from Eq. (19). It is specially interesting the port where the generator is connected, since it allows the knowing of the return losses of the whole structure, once the effects of the mutual coupling are included.

Table 1. Design details.

Slot	Offset [mm]	Length [mm]	P_{rad} [Norm.]	WG length
1	4.5	11.6	0.26	-
2	-4.3	12.6	0.24	$0.483\lambda_g$
3	3.7	11.8	0.27	$0.5\lambda_g$
4	-2.7	12	0.23	$0.538\lambda_g$

		Length [mm]
Short	$0.22126\lambda_g$	7.52

5. 4-ELEMENT ARRAY EXAMPLE

To clarify the procedure herein explained, a small uniformly fed linear array of four elements will be expressly designed and simulated. It is intended to verify the methodology by means of a design appart from standards, employing a non-tabulated rectangular waveguide: $a = 18.4\,\text{mm}$, $b = 9\,\text{mm}$. All the slots have a thickness and width of $t = 1.25\,\text{mm}$ and $w = 1\,\text{mm}$, respectively. The inclination angle is fixed to $\theta = 45°$.

As the first main step, initially neglecting the external coupling between elements, the preliminary array is created with these structural parameters using MoM-FMP [5, 6]. The array's details are shown in Table 1.

The complementary array of wired-fed slots on a infinite ground plane is excited with the desired amplitude distribution. Since slots' length, distribution and excitation are known, the coupling factor can be calculated as described in Section 4.1.3, obtaining a 4-by-4 admittance matrix. Then the scattering matrix of the free half-space subnetwork is calculated.

In line with coupling study, the original network is modified to account for the externally interchanged energy, transforming every two-port equivalent network into the new network explained in Subsection 4.1.1. From these, the admittance matrices of the new three-by-three networks and their corresponding scattering matrices are calculated.

As it can be seen in Fig. 11, all the interfaces are sequentially numbered, being the last two the short termination and the generator input. According to this, the global 26-by-26 scattering matrix and

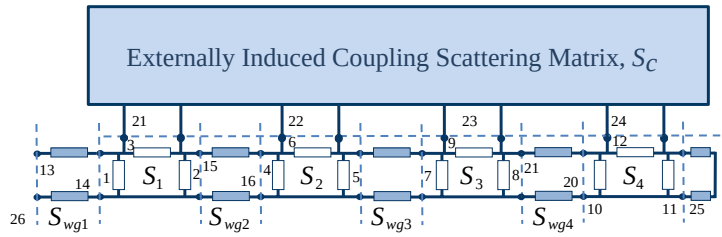

Figure 11. 4-Element array equivalent subnetworks.

the Γ connection matrix can be constructed:

$$S=\begin{bmatrix} S_{s1} & 0 & \dots & & 0 & \dots & 0 & \dots & & 0 & 0 \\ 0 & S_{s2} & 0 & \dots & \dots & 0 & & 0 & & & \\ \vdots & 0 & S_{S_3} & 0 & \dots & & 0 & \vdots & & \vdots & 0 \\ & \dots & 0 & S_{s_4} & 0 & \dots & \dots & & & 0 & \vdots \\ 0 & \dots & \dots & 0 & S_{wg_1} & 0 & \dots & \dots & & \vdots & \vdots \\ & 0 & \dots & \dots & 0 & S_{wg_2} & 0 & \dots & & & \vdots \\ \vdots & & \dots & & \dots & 0 & S_{wg_3} & \vdots & & 0 & \vdots \\ 0 & \dots & & \dots & 0 & \dots & 0 & S_{wg_4} & 0 & \vdots & \\ & 0 & \dots & 0 & \dots & & \dots & 0 & S_c & 0 & \vdots \\ & & & & & & & & & S_{short} & 0 \\ 0 & \dots & 0 & \dots & \dots & 0 & \dots & 0 & 0 & 0 & S_g \end{bmatrix} \tag{22}$$

where S_{S_i}, S_{wg_i} and S_c represent the scattering matrices of the i-slot, of the i-waveguide and the scattering matrix of the half-free subsystem, respectively. S_{short} and S_g are the reflection coefficients given at their corresponding ports.

The elements of Γ are all zero but those where two interfaces are connected which value is one.

At this point, from Eq. (19), Eq. (20) and Eq. (21) it is possible to predict the return loss of the global system.

$$\frac{b_g}{a_g} = \frac{b_{26}}{a_{26}} = S_{11} \tag{23}$$

In addition to this, since the coupling factors and array distribution are known, a prediction of the radiation pattern can also be calculated from the equivalent array of cable-fed slots. Both results are displayed in Fig. 12.

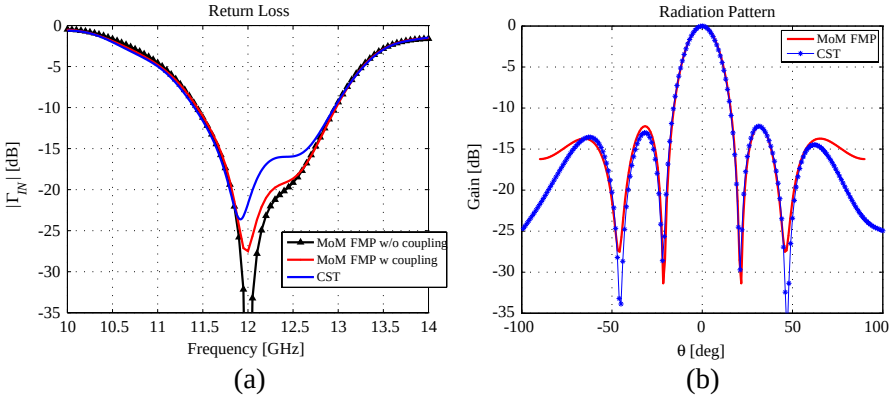

Figure 12. 4-element array performance. (a) Return loss. (b) Radiation pattern.

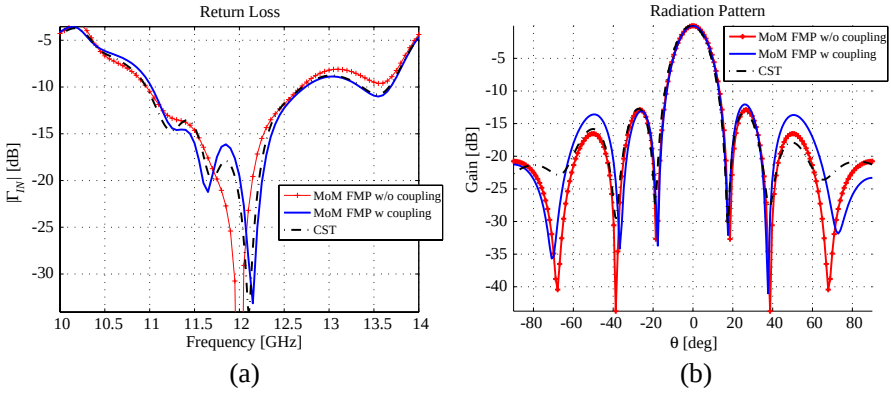

Figure 13. Reduced-height 5-element array performance. (a) Return loss. (b) Radiation pattern.

6. PRACTICAL RESULTS

In this section the predicted results in terms of input losses and radiation pattern of four different models obtained using MoM-FMP are compared to those given by CST Studio. It is supposed that the conductor has no losses and the slots are perfectly squared for all the processes here presented.

First, two arrays of 45°-tilted slots of twelve and five elements are presented. The working frequency for both of them is 12 GHz with an uniform aperture distribution. The first one is designed on a WR75 standard waveguide, $a = 19.05\,\text{mm}$, $b = 9.525\,\text{mm}$, with a conductor thickness of $t = 1.25\,\text{mm}$. For the second one, the array is

designed using a non-standard reduced-height rectangular waveguide, ($a = 19.55\,\text{mm}$, $b = 4.75\,\text{mm}$, $t = 1.25\,\text{mm}$). For this kind of arrays the amount of coupled power from the waveguide to the slot is bigger than for the normal-height waveguides and the effect of mutual coupling is more noticeable. This fact limits the number of elements that the array can consist of and prohibits abrupt tapers in the amplitude distribution.

The given solution by MoM-FMP without taking into account the surrounding elements is close to the results given by CST, but there was a noticeable difference around the working frequency where the perfect matching was supposedly achieved. After the inclusion of the mutual coupling effect, CST and MoM-FMP radiation and reflection

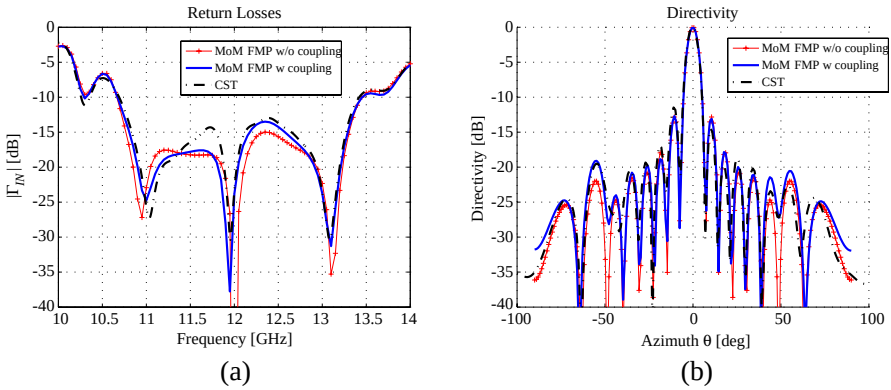

Figure 14. 12-element array performance. (a) Return loss. (b) Radiation pattern.

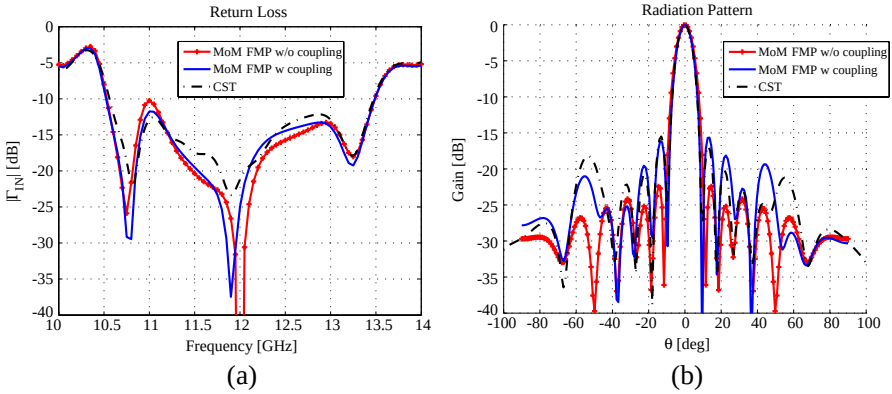

Figure 15. 25 dB-Taylor distribution 10-element array performance. (a) Return loss. (b) Radiation pattern.

results get closer and the frequency point of ideal matching disappears, Figs. 13(b) and 14(b).

The third proposed model is a 10-element array designed to have an ideal 25 dB Taylor distribution. The working frequency and waveguide characteristics are the same as in the first case. The arrays with a pronounced amplitude taper are very sensitive to the effects of mutual coupling as it is shown in this example, where the side-lobe level is increased comparing to the ideal case from −22.4 dBi to −15.8 dBi. In addition to this the main beam is narrowed, Fig. 15. Both effects are visible in the radiation pattern calculated by MoM-FMP and confirmed by CST.

7. CONCLUSION

A proven procedure for including the mutual coupling effects on the compound-slot array design is here presented. Existing methods cannot be applied and reasons are physically demonstrated. The employed circuit theory is explained and some different designed arrays' performances are shown. These are compared to results given my commercial solvers, where an excellent agreement is achieved.

ACKNOWLEDGMENT

Authors want to thank Ando and Hirokawa Laboratory staff at Tokyo Institute of Technology and the staff from Radiation Group at ETSI Telecomunicación at Universidad Politécnica de Madrid for their wholehearted support and help during the research period. Authors also thank the TERASENSE project (Consolider-Ingenio Program CSD 2008-068) and the SICOMORO project (TEC-2011-28789-C02-01) for their sponsorship.

REFERENCES

1. Elliott, R. S., *Antenna Theory and Design*, Wiley-IEEE Press, New York, 1981.
2. Elliott, R. S., "An improved design procedure for small arrays of shunt slots," *IEEE Trans. Antennas Propagat.*, Vol. 31, 48–53, 1983.
3. Gülick, J. J. and R. S. Elliott, "A general design procedure for small arrays of waveguide-fed slots," *Proc. of the Antennas And Propgat. Soc. Symp.*, 302–305, 1987.

4. Gülick, J. J., G, J. Stern, and R. S. Elliott, "The equivalent circuit of a rectangular-waveguide-fed longitudinal slot," *Proc. of the Antennas And Propgat. Soc. Symp.*, 685–688, 1986.
5. Montesinos-Ortego, I., M. Zhang, M. Sierra-Prez, J. Hirokawa, and M. Ando, "Systematic design methodology for one-dimensional compound slot-arrays combining method of moments, equivalent circuit model and forward matching procedure," *IEEE Trans. Antennas Propagat.*, Vol. PP, No. 99, 1, 2012, DOI: 10.1109/TAP.2012.2220108.
6. Montesinos-Ortego, I., M. Zhang, M. Sierra-Prez, J. Hirokawa, and M. Ando, "Study of the Π network as the compound slot equivalent circuit model," *Proc. of the 5th European Conf. on Antennas and Propagation*, 1186–1190, Rome, Italy, Apr. 11–15, 2011.
7. Rengarajan, S. R., "Efficient and accurate evaluation of external mutual coupling between compound broadwall slots," *IEEE Trans. Antennas Propagat.*, Vol. 40, No. 6, 734–737, 1992.
8. Silver, S., *Microwave Antenna Theory and Design*, MIT Radiation Lab. Series, McGraw Hill, London, 1949.
9. Gupta, K. C., *Computer-aided Design of Microwave Circuits*, Artech House, Massachusetts, 1981.
10. Collin, R. E., *Foundations of Microwave Engineering*, Wiley-IEEE Press, New York, 2000.
11. Kurokawa, K., "Power waves and the scattering matrix," *IEEE Trans. on Microwave Theory and Techniques*, 194–202, Mar. 1965.
12. Kakatkar, S. S. and K. P. Ray, "Evaluation of mutual coupling between slots from dipole expressions," *Progress In Electromagnetics Research M*, Vol. 9, 123–138, 2009.
13. Kakatkar, S. S. and K. P. Ray, "Near field of slot radiators," *Progress In Electromagnetics Research M*, Vol. 7, 41–55, 2009.
14. Richmond, J. H., "Mutual impedance between coplanar skew dipoles," *IEEE Trans. Antennas Propagat.*, Vol. 18, 414–416, 1970.